

Precision Spectroscopy and Nuclear Structure Parameters in ${}^7\text{Li}^+$ ion

Hua Guan^{1,*}, Xiao-Qiu Qi^{2,*}, Peng-Peng Zhou¹, Wei Sun^{5,1}, Shao-Long Chen¹,
Xu-Rui Chang^{1,7}, Yao Huang¹, Pei-Pei Zhang¹, Zong-Chao Yan^{3,1}, G. W. F.
Drake⁴, Ai-Xi Chen², Zhen-Xiang Zhong^{6,1}, Ting-Yun Shi^{1,†}, and Ke-Lin Gao^{1,‡}

¹State Key Laboratory of Magnetic Resonance and Atomic and Molecular Physics,
Wuhan Institute of Physics and Mathematics, Innovation Academy for Precision Measurement Science and Technology,
Chinese Academy of Sciences, Wuhan 430071, China

²Physics Department of Zhejiang Sci-Tech University, Hangzhou 310018, China

³Department of Physics, University of New Brunswick, Fredericton, New Brunswick, Canada E3B 5A3

⁴Department of Physics, University of Windsor, Windsor, Ontario, Canada N9B 3P4

⁵Key Laboratory of Green and High-end Utilization of Salt Lake Resources,
Qinghai Institute of Salt Lakes, Chinese Academy of Sciences, Xining 810008, China

⁶Center for Theoretical Physics, School of Physics and Optoelectronic
Engineering, Hainan University, Haikou 570228, China and

⁷University of Chinese Academy of Sciences, Beijing 100049, China

(Dated: March 12, 2024)

The optical Ramsey technique is used to obtain precise measurements of the hyperfine splittings in the 2^3S_1 and 2^3P_J states of ${}^7\text{Li}^+$. Together with bound-state quantum electrodynamic theory, the Zemach radius and quadrupole moment of the ${}^7\text{Li}$ nucleus are determined to be $3.35(1)$ fm and $-3.86(5)$ fm² respectively, with the quadrupole moment deviating from the recommended value of $-4.00(3)$ fm² by 1.75σ . Furthermore, we determine the quadrupole moment ratio of ${}^6\text{Li}$ to ${}^7\text{Li}$ as $0.101(13)$, exhibiting a 6σ deviation from the previous measured value of $0.020161(13)$ by LiF molecular spectroscopy. The results taken together provide a sensitive test of nuclear structure models.

Introduction.— The helium-like Li^+ ion is considered a fundamental atomic system due to its spectroscopic properties, encompassing fine and hyperfine structure (hfs), which can be experimentally measured and theoretically calculated with high precision. This system serves as a platform for testing bound-state quantum electrodynamics (QED) [1–5], determining nuclear properties [6–8], and exploring potential physics beyond the standard model [9]. Lithium has two stable isotopes, ${}^6\text{Li}$ and ${}^7\text{Li}$, each with nonzero nuclear spins exceeding $1/2$. This makes it an ideal subject for investigating nuclear structure, including the determination of the Zemach radius and nuclear quadrupole moment through atomic spectroscopy [10–12].

In recent theoretical work, Pachucki *et al.* computed the $m\alpha^7$ correction for the hyperfine structure of the 2^3S_1 state in ${}^6,7\text{Li}^+$ [13], resulting in a four-fold improvement in theoretical accuracy compared to previous calculations [11]. Additionally, they updated the values of the Zemach radii for ${}^6,7\text{Li}$ to be $2.39(2)$ fm and $3.33(3)$ fm, respectively. It is intriguing that the newly determined Zemach radius of ${}^6\text{Li}$ still does not align with the predicted value of $3.71(16)$ fm from nuclear models [14]. The disagreement is puzzling, especially considering the good agreement observed in the case of ${}^7\text{Li}$ [11].

Moreover, recent hyperfine structure measurements on the 2^3S_1 and 2^3P_J states of ${}^6\text{Li}^+$ have achieved a precision of 10 kHz [12]. An estimate from this of the nuclear quadrupole moment Q_d of ${}^6\text{Li}$ yielded $-0.38(20)$ fm² [12]. This value is in good agreement with $-0.35(6)$ fm² from a Greens function Monte Carlo calculation

[15, 16]. However, there is considerable divergence in the theoretical values, owing to a sensitive dependence on the details of the effective interaction, ranging from -0.061 fm² [17] and $-0.066(40)$ fm² [18] to $-0.35(6)$ fm². For example, the value -0.061 fm² from fermionic molecular dynamics calculations [17] becomes positive if the tensor part of the interaction is not included. The lower range agrees with the recommended experimental value $-0.0806(6)$ fm² [19, 20]. However, in contrast to our value based on hyperfine structure [12], this recommended value of Q_d for ${}^6\text{Li}$ is obtained from molecular spectroscopic methods by measuring the ratio $Q_d({}^6\text{Li})/Q_d({}^7\text{Li})$. In addition, the value of $Q_d({}^7\text{Li}) = -4.00(3)$ fm² primarily relies on the analysis from molecular beam magnetic resonance experiments [20–22].

Hence, we aim to determine the Zemach radius and nuclear quadrupole moment of ${}^7\text{Li}^+$ through improved high-precision measurements of its hyperfine structure in order to obtain an independent measure of the ratio $Q_d({}^6\text{Li})/Q_d({}^7\text{Li})$.

Hyperfine structure refers to the additional splitting of atomic energy levels caused by nuclear spin. Figure 1 shows a schematic diagram illustrating the energy levels of ${}^7\text{Li}^+$, where the hyperfine structure is displaced in addition to the fine structure. The hyperfine level splitting can be expressed as

$$E_{\text{hfs}} = E_p + E_{\text{ZM}} + E_{Q_d}, \quad (1)$$

where E_p represents the energy of hfs obtained for the case of a point nucleus, and E_{ZM} and E_{Q_d} are contributions generated by the nuclear Zemach radius [23]

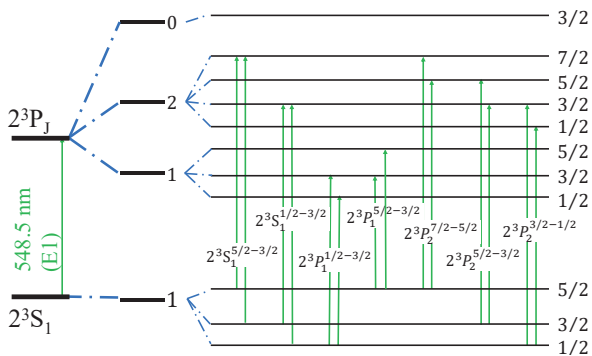


FIG. 1. Fine and hyperfine structures for the 2^3S_1 and 2^3P_J states of ${}^7\text{Li}^+$ ion (not to scale).

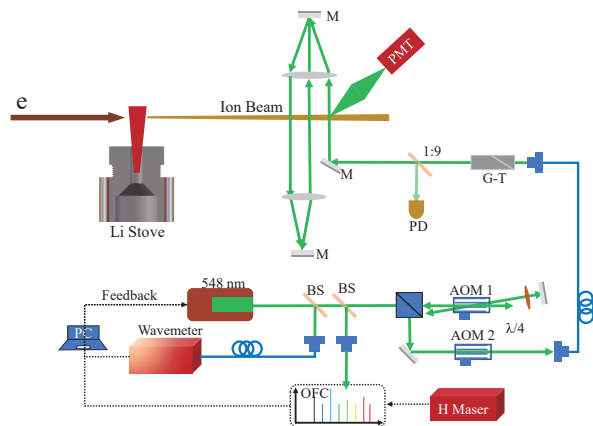


FIG. 2. The experimental setup. M: Mirror, BS: Beam Splitter, PD: Photodetector, G-T: Glan-Taylor, AOM: Acousto-Optic Modulator, PMT: Photomultiplier, OFC: Optical Frequency Comb.

and quadrupole moment, respectively. Since the nuclear quadrupole moment does not contribute to the 2^3S_1 state, we can extract the Zemach radius by experimentally measuring the hfs of the 2^3S_1 state. Subsequently, the obtained Zemach radius and corresponding experimental measurements of the 2^3P_J state are utilized to determine the nuclear quadrupole moment.

Experiment.— The present hfs measurements rely on the optical Ramsey technique [24–26] employing separated laser fields. The experimental setup is depicted in Figure 2. A more comprehensive account of the ion source and the corresponding laser systems for the separated fields can be found in Refs. [12, 27]. Here, a concise description is provided. The collimated ${}^7\text{Li}^+$ ion beam interacts with three consecutive equally spaced standing-wave light fields and remains unconfined in the region between the laser beams. The Ramsey interference spectroscopy is probed by scanning the laser frequency using Acousto-Optic Modulator 1 (AOM 1), with the fluorescence of ions serving as the detection signal. Concur-

rently, the probe laser frequency is precisely stabilized using a high-precision wavemeter (WS-7 HighFinesse) and an optical frequency comb (FC8004, Menlosystems) via a digital feedback method, ensuring its suitability for long-term measurements [28]. The wavemeter is regularly calibrated, and the optical frequency comb is referenced to a hydrogen maser (CHI-75A, Kvarz). The central frequency of the spectrum is determined by fitting the data set with a suitable function. The hfs is determined by measuring two neighboring transition frequencies with a common upper or lower energy level. Each hfs is measured 100 – 200 times over a period of 10 hours, from which the statistical mean and uncertainty listed in Table I are calculated.

During the energy level splitting measurement, systematic effects that impact the spectroscopy frequency are common to both optical transitions, effectively canceling each other out. The evaluation of systematic errors, such as Doppler shift, laser power, Zeeman effect, and quantum interference, has been extensively discussed in our previous studies [12]. Their contributions in this work are similar and are listed in Table I. For a detailed description, see the Supplemental Material [29] and our previous work [12].

Results and discussion.— Table II provides a comparison of our final measured hyperfine splittings with both previous experimental findings and theoretical calculations. Our results showcase a four-fold increase in accuracy for the 2^3S_1 state compared to prior experimental data, and a five to ten-fold increase in accuracy for the 2^3P_J state. As shown in the last row by the root-mean-square deviations $\bar{\Delta}$ between theory and experiment, these improved values align much more closely with the theoretical calculations [11] in the last column. Our results can be used to derive more precise values for the Zemach radius and electric quadrupole moment of the ${}^7\text{Li}$ nucleus.

We first consider the 2^3S_1 state, where the contribution of the nuclear quadrupole moment vanishes. The hfs can thus be expressed in the form [10, 13, 34]

$$E_{\text{hfs}}(2^3S_1) = E_F(1 + \delta_{\text{HO}}), \quad (2)$$

where $E_F = A(\mathbf{I} \cdot \mathbf{S})$ is the Fermi contact term [11], A is the hyperfine constant, \mathbf{I} is the nuclear spin, and \mathbf{S} is the total electron spin. Also in the above, the higher-order correction δ_{HO} is given by

$$\delta_{\text{HO}} = a_e + \delta_{\text{QED}} + \delta_{\text{ZM}}, \quad (3)$$

where a_e is the anomalous magnetic moment of the electron, δ_{QED} is a sum of higher-order QED corrections, and δ_{ZM} is the contribution of the Zemach radius. For the Zemach radius, we use the effective radius \tilde{R}_{em} recently introduced by Pachucki *et al.* [13] to account for other nuclear structure effects that would otherwise be omitted. It is defined by

$$\delta_{\text{ZM}} = -2Z\tilde{R}_{\text{em}}/a_0, \quad (4)$$

TABLE I. Experimental results for the hfs intervals of the 2^3S_1 and 2^3P_J states of ${}^7\text{Li}^+$ with uncertainty budget, in kHz.

Source of error	$2^3S_1^{1/2-3/2}$	$2^3S_1^{3/2-5/2}$	$2^3P_1^{1/2-3/2}$	$2^3P_1^{3/2-5/2}$	$2^3P_2^{1/2-3/2}$	$2^3P_2^{3/2-5/2}$	$2^3P_2^{5/2-7/2}$
Statistics	11890011(7)	19817676(6)	4238968(5)	9966436(5)	6203320(5)	9608237(4)	11773065(4)
First-order Doppler	(3.2)	(3.2)	(3.2)	(3.2)	(3.2)	(3.2)	(3.2)
Second-order Doppler	0.90(5)	1.51(8)	0.32(2)	0.76(4)	0.47(2)	0.73(4)	0.90(5)
Laser power	(5.0)	(5.0)	(5.0)	(5.0)	(5.0)	(5.0)	(5.0)
Zeeman effect	(8.48)	(3.19)	(6.7)	(3.3)	(8.9)	(3.18)	(0.33)
Quantum interference	(8)	(8)	(8)	(8)	(8)	(8)	(8)
Total	11890012(15)	19817677(12)	4238968(13)	9966437(11)	6203320(14)	9608238(11)	11773066(11)

TABLE II. Experimental and theoretical hyperfine intervals in the 2^3S_1 and 2^3P_J states of ${}^7\text{Li}^+$, in MHz. $\overline{\Delta}(2^3P)$ represents the root-mean-square deviation of the other results from the theoretical values of Qi *et al.* [11].

hfs interval	Experiment				Theory	
	Kötz <i>et al.</i> [30, 31]	Clarke <i>et al.</i> [32]	Guan <i>et al.</i> [33]	This work	Drake <i>et al.</i> [34]	Qi <i>et al.</i> [11]
$2^3S_1^{1/2-3/2}$	11890.018(40)	11891.22(60)	11890.088(65)	11890.012(15)	11890.013(38)	
$2^3S_1^{3/2-5/2}$	19817.673(40)	19817.90(93)	19817.696(42)	19817.677(12)	19817.680(25)	
$2^3P_1^{1/2-3/2}$	4237.8(10)	4239.11(54)	4238.823(111)	4238.968(13)	4238.86(20)	4238.920(49)
$2^3P_1^{3/2-5/2}$	9965.2(6)	9966.30(69)	9966.655(102)	9966.437(11)	9966.14(13)	9966.444(34)
$2^3P_2^{1/2-3/2}$	6203.6(5)	6204.52(80)	6203.319(67)	6203.320(14)	6203.27(30)	6203.408(95)
$2^3P_2^{3/2-5/2}$	9608.7(20)	9608.90(49)	9608.220(54)	9608.238(11)	9608.12(15)	9608.311(54)
$2^3P_2^{5/2-7/2}$	11775.8(5)	11774.04(94)	11772.965(74)	11773.066(11)	11773.05(18)	11773.003(55)
$\overline{\Delta}(2^3P)$	1.47	0.74	0.12	0.06	0.18	

TABLE III. The determination of the Zemach radius contribution δ_{ZM} by the hfs of the 2^3S_1 state and the effective Zemach radius \tilde{R}_{em} (in fm).

Term	Value
A_{the} (kHz) [13]	7917508.1(1.3)
A_{exp} (kHz)	7926971.8(4.4)
$a_e + \delta_{\text{QED}}$ [13]	0.0015749(5)
$\delta_{\text{HO}} = A_{\text{exp}}/A_{\text{the}} - 1$	0.0011953(6)
δ_{ZM}	-0.0003796(8)
\tilde{R}_{em} (this work)	3.35(1)
\tilde{R}_{em} [13]	3.33(3)
\tilde{R}_{em} [11]	3.38(3)
\tilde{R}_{em} [10]	3.23(4)

where Z is the nuclear charge and a_0 the Bohr radius.

Here, we use the method introduced by Pachucki *et al.* [13] to calculate the hyperfine constant A , which has a conversion relationship with the hfs of the 2^3S_1 state:

$$A = \frac{1}{6}\nu_{1/2-3/2} + \frac{3}{10}\nu_{3/2-5/2}. \quad (5)$$

Combining the experimentally extracted value of A_{exp} with the theoretically calculated value of A_{the} , we can determine the contribution of δ_{HO} . Furthermore, by separating the contributions of the anomalous magnetic moment and QED parts, we can obtain the value of δ_{ZM} . The contribution of the Zemach radius δ_{ZM} and the determined effective Zemach radius \tilde{R}_{em} are presented in

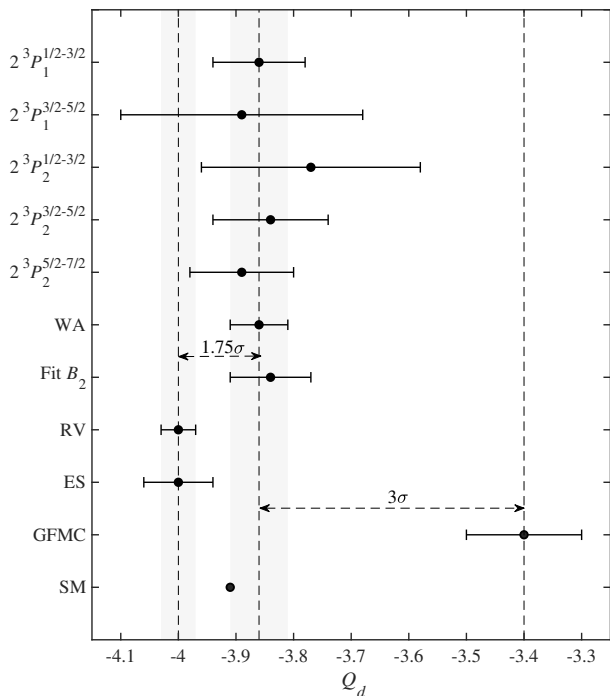


FIG. 3. The nuclear quadrupole moment Q_d of ${}^7\text{Li}$, in fm^2 . WA: Weighted Average, RV: Recommended Value [20], Fit B_2 : Determined from fitting B_2 , ES: Electron Scattering [35], GFMC: Greens function Monte Carlo [15, 16], SM: Shell Model [36].

TABLE IV. Determination of the nuclear quadrupole moments Q_d of ${}^7\text{Li}^+$ using the 2^3P_J state hfs, where $R_{\text{em}} = 3.35(1)$ fm is adopted. In the table, ν_{exp} represents the experimentally measured hfs from this work, and $\nu(0)$, X , and Y are theoretically calculated values.

hfs interval	ν_{exp} kHz	$\nu(0)$ kHz	X kHz/fm ²	$10^4 Y$ kHz/fm ⁴	$10^4 Y Q_d^2$ kHz	Q_d fm ²
$2^3P_1^{1/2-3/2}$	4238968(13)	4240834(36)	483.335	-0.0583	0.9	-3.86(8)
$2^3P_1^{3/2-5/2}$	9966437(11)	9965928(25)	-130.852	11.2667	170.7	-3.89(21)
$2^3P_2^{1/2-3/2}$	6203320(14)	6201910(70)	-373.765	-14.2361	202.6	-3.77(19)
$2^3P_2^{3/2-5/2}$	9608238(11)	9606562(40)	-436.891	3.0277	44.6	-3.84(10)
$2^3P_2^{5/2-7/2}$	11773066(11)	11774902(40)	472.064	-8.2469	124.8	-3.89(9)
Weighted Average (WA)						-3.86(5)
Fit B_2 [29]						-3.84(7)
Recommended Value (RV) [20]						-4.00(3)
Electron Scattering (ES) [35]						-4.00(6)
Greens function Monte Carlo (GFMC) [15, 16]						-3.4(1)
Shell Model (SM) [36]						-3.91

Table III. Our latest result for the effective Zemach radius is in agreement with previous values, with a three-fold increase in accuracy.

Next, we employ a Taylor expansion to directly analyze the impact of the quadrupole moment Q_d on the hfs of the 2^3P_J state [37]:

$$\nu(Q_d) = \nu(0) + XQ_d + YQ_d^2 + O(Q_d^3), \quad (6)$$

where $\nu(0)$ is the hfs without Q_d , and its theoretical calculation has been discussed in detail in our previous work (see Ref. [11] and its Supplemental Material). In the next term, X is the linear expansion coefficient independent of Q_d that can be evaluated through the first-order derivative of $\nu(Q_d)$ at $Q_d = 0$. The quadratic term in the equation is used to evaluate the magnitude of higher-order contributions and determine whether retaining the linear term is sufficient at the current accuracy.

Table IV displays the results for our calculated values of $\nu(0)$, X , and Y corresponding to five hyperfine transitions. These values, in conjunction with our measured hyperfine structure frequency ν_{exp} , enable the extraction of the nuclear quadrupole moment Q_d . It is evident that higher-order contributions of Q_d are anticipated to be smaller than 0.01 kHz, which can be ignored compared to the current level of precision. The extracted values for Q_d exhibit agreement among themselves, as plotted in Figure 3. The final determination, $Q_d = -3.86(5)$ fm², is derived through a weighted average of the five Q_d values, resulting in an accuracy of approximately 1%. The disparity between this result and the current recommended literature value, $Q_d = -4.00(3)$ fm², amounts to 1.75σ . Our result also differs significantly from the value obtained through the Greens function Monte Carlo method by 3σ , yet it aligns with the value obtained by the Shell Model.

Additionally, we employed the method of Pachucki *et al.* [38] to compute the hyperfine constants A_J , B_J , and C_J for the 2^3P_J state, as detailed in the Supplemental

Material [29]. This method facilitated the extraction of the nuclear quadrupole moment of ${}^7\text{Li}$ as $-3.84(7)$ fm² through the fitting of B_2 . Both extracted values are found to be consistent with each other.

By incorporating $Q_d({}^6\text{Li}) = -0.39(5)$ fm², as obtained from our earlier study [12] with adjustments made for errors [29], we have computed the ratio $Q_d({}^6\text{Li})/Q_d({}^7\text{Li}) = 0.101(13)$. As stated in the Introduction, this ratio shows a substantial deviation from the value 0.020161(13) derived from the molecular hyperfine spectra of ${}^6\text{Li}^{19}\text{F}$ and ${}^7\text{Li}^{19}\text{F}$ [19]. However, the ${}^6\text{Li}$ result is consistent with the larger theoretical value $Q_d = -0.35(6)$ fm² from the Greens function Monte Carlo calculation [15, 16], rather than the smaller values (in absolute magnitude) of -0.061 fm² [17] and $-0.066(40)$ fm² [18].

Conclusion.— The $2^3S_1-2^3P_J$ transitions of ${}^7\text{Li}^+$ were investigated using the optical Ramsey technique, resulting in highly precise determinations of the hyperfine splittings for the 2^3S_1 and 2^3P_J states. These new findings substantially decrease the uncertainties of prior experiments, and they demonstrate improved agreement with theoretical values. By combining the measured hyperfine intervals of the 2^3S_1 state with the latest quantum electrodynamic calculations, we have tripled the accuracy of the Zemach radius of the ${}^7\text{Li}$ nucleus. Using such determined Zemach radius and hyperfine structure of the 2^3P_J state, we determined the nuclear quadrupole moment of ${}^7\text{Li}$, which deviates from the recommended Q_d value [20] and the Greens function Monte Carlo value [15, 16] by 1.75σ and 3σ , respectively. Finally, we computed the ratio $Q_d({}^6\text{Li})/Q_d({}^7\text{Li})$, which significantly differs from the LiF molecular spectroscopy measurement. These discrepancies are perplexing, and we call for additional experimental measurements in atomic and molecular spectroscopy, electron scattering, and related theoretical calculations pertaining to lithium.

The authors thank Qunfeng Chen, Yanqi Xu, and

Huanyao Sun for technical support in optical frequency comb and electronic circuits. We also thank Liyan Tang and Fangfei Wu for helpful discussions regarding the assessment of systematic errors. This work is supported jointly by the National Natural Science Foundation of China (Grants No. 11934014, No. 92265206, No. 12393823, No. 12393821, No. 12121004, No. 12274423, No. 12204412, No. 12175199, No. 11974382, and No. 12174400), CAS Project for Young Scientists in Basic Research (Grant No. YSBR-085 and No. YSBR-055), Natural Science Foundation of Hubei Province (Grant No. 2022CFA013), Science Foundation of Zhejiang Sci-Tech University (Grant No. 21062349-Y), CAS Youth Innovation Promotion Association (Grants No. Y2022099). Z. C. Y. and G. W. F. D. acknowledge research support by the Natural Sciences and Engineering Research Council of Canada.

*These authors contributed equally to this work.

†Email Address: tyshi@wipm.ac.cn

‡Email Address: klgaow@wipm.ac.cn

-
- [1] Z.-C. Yan and G. W. F. Drake, High precision calculation of fine structure splittings in helium and He-like ions, *Phys. Rev. Lett.* **74**, 4791 (1995).
- [2] Z.-C. Yan, W. Nörtershäuser, and G. W. F. Drake, High precision atomic theory for Li and Be⁺: QED shifts and isotope shifts, *Phys. Rev. Lett.* **100**, 243002 (2008).
- [3] K. Pachucki and V. A. Yerokhin, Fine structure of heliumlike ions and determination of the fine structure constant, *Phys. Rev. Lett.* **104**, 070403 (2010).
- [4] V. c. v. Patkóš, V. A. Yerokhin, and K. Pachucki, Complete quantum electrodynamic $\alpha^6 m$ correction to energy levels of light atoms, *Phys. Rev. A* **100**, 042510 (2019).
- [5] F.-F. Wu, K. Deng, and Z.-H. Lu, Tune-out wavelengths for the 2^3S_1 state of the Li⁺ ion, *Phys. Rev. A* **106**, 042816 (2022).
- [6] R. Neugart, D. L. Balabanski, K. Blaum, D. Borremans, P. Himpe, M. Kowalska, P. Lievens, S. Mallion, G. Neyens, N. Vermeulen, and D. T. Yordanov, Precision measurement of ¹¹Li moments: Influence of halo neutrons on the ⁹Li core, *Phys. Rev. Lett.* **101**, 132502 (2008).
- [7] Z.-T. Lu, P. Mueller, G. W. F. Drake, W. Nörtershäuser, S. C. Pieper, and Z.-C. Yan, Colloquium: Laser probing of neutron-rich nuclei in light atoms, *Rev. Mod. Phys.* **85**, 1383 (2013).
- [8] X. Yang, S. Wang, S. Wilkins, and R. G. Ruiz, Laser spectroscopy for the study of exotic nuclei, *Progress in Particle and Nuclear Physics* **129**, 104005 (2023).
- [9] G. W. F. Drake, H. S. Dhindsa, and V. J. Marton, King and second-king plots with optimized sensitivity for lithium ions, *Phys. Rev. A* **104**, L060801 (2021).
- [10] M. Puchalski and K. Pachucki, Ground state hyperfine splitting in ^{6,7}Li atoms and the nuclear structure, *Phys. Rev. Lett.* **111**, 243001 (2013).
- [11] X.-Q. Qi, P.-P. Zhang, Z.-C. Yan, G. W. F. Drake, Z.-X. Zhong, T.-Y. Shi, S.-L. Chen, Y. Huang, H. Guan, and K.-L. Gao, Precision calculation of hyperfine structure and the zemach radii of ^{6,7}Li⁺ ions, *Phys. Rev. Lett.* **125**, 183002 (2020).
- [12] W. Sun, P.-P. Zhang, P.-p. Zhou, S.-l. Chen, Z.-q. Zhou, Y. Huang, X.-Q. Qi, Z.-C. Yan, T.-Y. Shi, G. W. F. Drake, Z.-X. Zhong, H. Guan, and K.-l. Gao, Measurement of hyperfine structure and the zemach radius in ⁶Li⁺ using optical ramsley technique, *Phys. Rev. Lett.* **131**, 103002 (2023).
- [13] K. Pachucki, V. c. v. Patkóš, and V. A. Yerokhin, Hyperfine splitting in ^{6,7}Li⁺, *Phys. Rev. A* **108**, 052802 (2023).
- [14] V. A. Yerokhin, Hyperfine structure of Li and Be⁺, *Phys. Rev. A* **78**, 012513 (2008).
- [15] S. C. Pieper and R. B. Wiringa, Quantum monte carlo calculations of light nuclei, *Annual Review of Nuclear and Particle Science* **51**, 53 (2001).
- [16] S. C. Pieper, K. Varga, and R. B. Wiringa, Quantum monte carlo calculations of $A = 9, 10$ nuclei, *Phys. Rev. C* **66**, 044310 (2002).
- [17] W. Nörtershäuser, T. Neff, R. Sánchez, and I. Sick, Charge radii and ground state structure of lithium isotopes: Experiment and theory reexamined, *Phys. Rev. C* **84**, 024307 (2011).
- [18] C. Forssén, E. Caurier, and P. Navrátil, Charge radii and electromagnetic moments of Li and Be isotopes from the ab initio no-core shell model, *Phys. Rev. C* **79**, 021303 (2009).
- [19] J. Cederberg, D. Olson, J. Larson, G. Rakness, K. Jarausch, J. Schmidt, B. Borovsky, P. Larson, and B. Nelson, Nuclear electric quadrupole moment of ⁶Li, *Phys. Rev. A* **57**, 2539 (1998).
- [20] N. Stone, Table of nuclear electric quadrupole moments, *At. Data Nucl. Data Tables* **111-112**, 1 (2016).
- [21] L. Wharton, L. P. Gold, and W. Klemperer, Quadrupole moment of ⁶Li, *Phys. Rev.* **133**, B270 (1964).
- [22] P. Pyykkö, Year-2008 nuclear quadrupole moments, *Molecular Physics* **106**, 1965 (2008).
- [23] A. C. Zemach, Proton structure and the hyperfine shift in hydrogen, *Phys. Rev.* **104**, 1771 (1956).
- [24] Y. V. Baklanov, B. Y. Dubetsky, and V. Chebotayev, Non-linear ramsley resonance in the optical region, *Applied physics* **9**, 171 (1976).
- [25] C. J. Bordé, C. Salomon, S. Avrillier, A. van Lerberghe, C. Bréant, D. Bassi, and G. Scoles, Optical ramsley fringes with traveling waves, *Phys. Rev. A* **30**, 1836 (1984).
- [26] J. C. Bergquist, S. A. Lee, and J. L. Hall, Saturated absorption with spatially separated laser fields: Observation of optical “Ramsey” fringes, *Phys. Rev. Lett.* **38**, 159 (1977).
- [27] S. Chen, S. Liang, W. Sun, Y. Huang, H. Guan, and K. Gao, Saturated fluorescence spectroscopy measurement apparatus based on metastable Li⁺ beam with low energy, *Review of Scientific Instruments* **90** (2019).
- [28] P. Zhou, W. Sun, S. Liang, S. Chen, Z. Zhou, Y. Huang, H. Guan, and K. Gao, Digital long-term laser frequency stabilization with an optical frequency comb, *Applied Optics* **60**, 6097 (2021).
- [29] See Supplemental Material at <http://link.aps.org/supplemental/> ??? for details of experimental measurement and theoretical analysis, which includes Refs. [??-??].
- [30] U. Kötz, J. Kowalski, R. Neumann, S. Noehte, H. Suhr, K. Winkler, and G. zu Putlitz, Laser-microwave spectroscopy of lithium ions: 2^3S_1 hyperfine structure of ⁷Li⁺, *Z. Phys. A* **300**, 25 (1981).

- [31] J. Kowalski, R. Neumann, S. Noehte, K. Scheffzek, H. Suhr, and G. zu Putlitz, Laser-microwave spectroscopy in the excited $1s2s^3S_1$ and $1s2p^3P$ hyperfine multiplets of helium-like $^{6,7}\text{Li}^+$, *Hyp. Int.* **15**, 159 (1983).
- [32] J. J. Clarke and W. A. van Wijngaarden, Hyperfine and fine-structure measurements of $^{6,7}\text{Li}^+1s2s^3S$ and $1s2p^3P$ states, *Phys. Rev. A* **67**, 012506 (2003).
- [33] H. Guan, S. Chen, X.-Q. Qi, S. Liang, W. Sun, P. Zhou, Y. Huang, P.-P. Zhang, Z.-X. Zhong, Z.-C. Yan, G. W. F. Drake, T.-Y. Shi, and K. Gao, Probing atomic and nuclear properties with precision spectroscopy of fine and hyperfine structures in the $^7\text{Li}^+$ ion, *Phys. Rev. A* **102**, 030801(R) (2020).
- [34] E. Riis, A. G. Sinclair, O. Poulsen, G. W. F. Drake, W. R. C. Rowley, and A. P. Levick, Lamb shifts and hyperfine structure in $^6\text{Li}^+$ and $^7\text{Li}^+$: Theory and experiment, *Phys. Rev. A* **49**, 207 (1994).
- [35] H.-G. Voelk and D. Fick, The electric moments of ^7Li from coulomb scattering, *Nucl. Phys. A* **530**, 475 (1991).
- [36] R. A. Radhi, Z. A. Dakhil, and N. S. Manie, Microscopic calculations of quadrupole moments in Li and B isotopes, *Eur. Phys. J A* **50**, 115 (2014).
- [37] X.-Q. Qi, P.-P. Zhang, Z.-C. Yan, T.-Y. Shi, G. W. F. Drake, A.-X. Chen, and Z.-X. Zhong, Theoretical hyperfine splittings of $^{7,9}\text{Be}^{2+}$ ions for future studies of nuclear properties, *Phys. Rev. A* **107**, L010802 (2023).
- [38] M. Puchalski, J. Komasa, and K. Pachucki, Hyperfine structure of the 2^3P state in ^9Be and the nuclear quadrupole moment, *Phys. Rev. Res.* **3**, 013293 (2021).